JACS
JOURNAL OF THE AMERICAN CHEMICAL SOCIETY
Communication
pubs.acs.org/JACS

Electrochemically Seed-Mediated Synthesis of Sub-10 nm Tetrahexahedral Pt Nanocrystals Supported on Graphene with Improved Catalytic Performance

Shuo Liu,[†] Na Tian,[*,†] Ai-Yun Xie,[†] Jia-Huan Du,[†] Jing Xiao,[†] Li Liu,[†] Hong-Yu Sun,[‡] Zhi-Ying Cheng,[‡] Zhi-You Zhou,[†] and Shi-Gang Sun[*,†]

[†]State Key Laboratory of Physical Chemistry of Solid Surfaces, Collaborative Innovation Center of Chemistry for Energy Materials, Department of Chemistry, College of Chemistry and Chemical Engineering, Xiamen University, Xiamen 361005, China

[‡]National Center for Electron Microscopy in Beijing, School of Materials Science and Engineering, Tsinghua University, Beijing 100084, People's Republic of China

Supporting Information

ABSTRACT: Controlling the surface structure of Pt nanocrystals (NCs), especially creating high-index facets with abundant active step sites, is an effective approach to enhance catalytic performances. However, the available high-index faceted Pt NCs have large particle sizes, which severely impedes their practical applications. In this study, we reported a new electrochemically seed-mediated method, by which sub-10 nm tetrahexahedral Pt NCs (THH Pt NCs) enclosed with {210} high-index facets supported on graphene were synthesized. Pt nanoparticles of ~3 nm in size as high-density crystal seeds play a key role in the small-sized control. The obtained THH Pt NCs exhibited a higher mass activity than commercial Pt/C catalyst for ethanol electrooxidation. We further demonstrated that this method is also valid for reshaping commercial Pt/C, to create high-index facets on surfaces and thus to improve both mass activity and stability.

Controlling surface structures (or crystal shapes) and particle sizes are two main approaches to improve the performance of Pt catalysts.[1,2] Low-coordinated surface sites such as step, edge, and corner atoms on nanoparticles exhibit high catalytic activities.[3] However, the fraction of these active sites on a nanoparticle is quite low because most surface atoms are smooth facet sites. Previously, we developed an electrochemical square-wave potential (SWP) method by which Pt-group metal nanocrystals (NCs) with high-index facets, such as tetrahexahedral Pt NCs (THH Pt NCs),[4] can be synthesized.[5] An unique feature of these NCs consists in that abundant step atoms also exist on the facets besides edges and corners; as a result, a high area-specific catalytic activity was observed. Thereafter, surfactant-based wet-chemical methods were also developed in other groups to synthesize NCs with high-index facets.[6] However, small-size (<10 nm) controlled synthesis is still a challenge. As catalytic reactions only occur on surfaces, large THH Pt NCs yield lower Pt utilization efficiency and mass activity than commercial Pt catalysts.[5b,7]

The challenge of electrochemical synthesis of sub-10 nm THH Pt NCs comes from the following aspect: high-index facets have very high surface energy, and they are formed through repetitive oxygen adsorption/desorption induced by SWP. However, under this condition, Pt crystal nuclei are easily dissolved. Although some crystal nuclei can survive, they quickly grow beyond 10 nm within dozens of seconds. In such a short time, high-index facets have not formed through repetitive oxygen adsorption/desorption. Hence, the insufficient amount of crystal nuclei is a key factor that impedes the electrochemical synthesis of small THH Pt NCs.

Herein, we reported an electrochemically seed-mediated method and synthesized sub-10 nm THH Pt NCs with {210} high-index facets supported on graphene. Pt nanoparticles (3.2 nm) supported on graphene were used as high-density crystal seeds, and their growth into THH Pt NCs was achieved via electrochemical SWP method. The obtained THH Pt NCs exhibited a higher mass activity than commercial Pt/C for ethanol electrooxidation. This method is also valid to reshape commercial Pt/C to improve both mass activity and stability.

Figure 1a,b illustrates the electrochemically seed-mediated synthesis of sub-10 nm THH Pt NCs. Pt nanoparticles (3.2 ± 0.6 nm) synthesized through $NaBH_4$ reduction from H_2PtCl_6 and supported on graphene without using surfactant were used as starting materials (Figure 1c, denoted as Pt/G). The commercial graphene used here contained some graphene oxide according to physical characterization of XPS, XRD, and FTIR (Figure S1). Pt/G can provide a much higher density of crystal seeds than those generated through direct electrodeposition. High-density crystal seeds will decrease the growth rate to THH Pt NCs and benefit the small-sized synthesis. Pt/G was dispersed onto a glassy carbon electrode and then subjected to an electrochemical SWP treatment for 150 s in a dilute Pt plating solution of 10 μM H_2PtCl_6 + 0.1 M H_2SO_4. The lower limit potential (E_L) of SWP was −0.30 V (vs SCE, i.e., saturated calomel electrode), the upper limit potential (E_U) was 1.11 V, and the frequency was 10 Hz. Figure 1d shows transmission electron microscopic (TEM) image of the obtained THH Pt NCs supported on graphene (denoted as THH-Pt/G). The Pt NCs were polyhedral, as indicated by an amplified TEM image with a hexagonal profile (the inset to Figure 1d). The average size of Pt NCs was 9.5 ± 0.7 nm. The yield of the THH Pt NCs among whole particles is

Received: December 25, 2015
Published: April 11, 2016

DOI: 10.1021/jacs.5b13473
J. Am. Chem. Soc. 2016, 138, 5753−5756

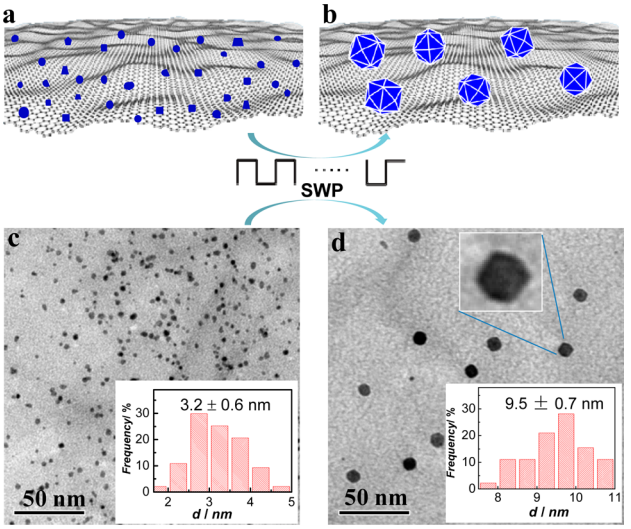

Figure 1. Illustration (a,b) and TEM images (c,d) of sub-10 nm THH Pt NCs synthesized via an electrochemically seed-mediated method. Pt nanoparticles (3.2 nm) supported on graphene were used as crystal seeds and then grew into THH Pt NCs (9.5 nm) through an electrochemical square-wave potential treatment in a dilute Pt plating solution (10 μM H_2PtCl_6 + 0.1 M H_2SO_4). The inset of high-magnification TEM image of THH Pt NCs in (d) shows a hexagonal profile.

larger than 90% (Figure S2), and the density of the THH Pt NCs is much lower than that of the starting Pt nanoparticles. This feature indicates that most of the Pt nanoparticle seeds have been dissolved during the SWP treatment.

The surface structure of THH Pt NCs was identified through TEM. Previously, we captured TEM image of THH Pt NC along the ⟨100⟩ crystal direction to determine the Miller indices of the facets.[4] In this direction, THH Pt NC will form an octagonal projection. However, when the particle size is less than 10 nm, it is difficult to distinguish whether the TEM image profile is an octagon formed by THH NC or a circle formed by common spherical nanoparticle (Figure S3) because the vertices of NCs are usually not perfect.[8] In this case, the ⟨110⟩ direction is a better choice because the projection of a THH NC along ⟨110⟩ direction is a hexagon that is easier to be distinguished from a circle than an octagon. Figure 2c illustrates an aberration-corrected high-resolution TEM (HRTEM) image of a THH Pt NC along [01$\bar{1}$] zone axis, as confirmed by fast Fourier transform (FFT) pattern (inset to Figure 2c). The HRTEM image exhibited a hexagonal profile as expected. The Miller indices of the exposed facets were determined by carefully measuring the TEM projection angles of α and β through the statistics of tens of THH Pt NCs (Figure S4). The measured values were α = 140.1 ± 2.0° and β = 109.9 ± 1.3°, which are consistent with the theoretical values of {210} facets (α = 141.06° and β = 109.47°). This result indicates that the surfaces of THH Pt NCs are mainly {210} facets.[9] The {210} facet is a stepped surface that composes of a two-atomic width (100) terrace followed by a monatomic (110) step (Figure S5).

The common cuboctahedral NC enclosed with {111} and {100} facets also displays a hexagonal projection along the ⟨110⟩ direction (Figure 2b–d). However, its hexagonal orientation is different from that of THH NCs. Both the (111) and (100) lattices of the cuboctahedral NC tend to form an edge along [111] and [100] directions, corresponding to {111} and {100} facets on the surfaces, respectively (Figure 2d). By contrast, both

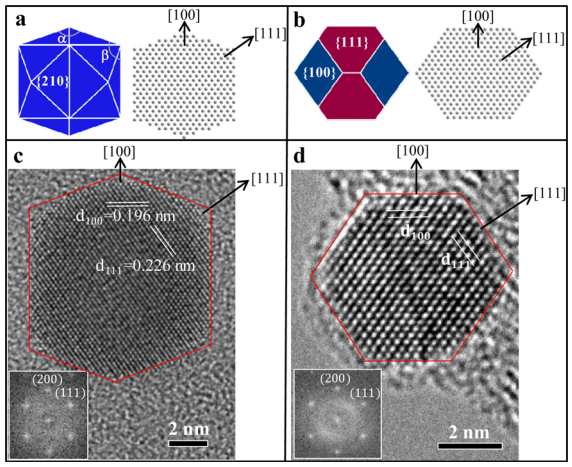

Figure 2. Model and aberration-corrected HRTEM images of THH-Pt/G (a,c) and common cuboctahedral Pt nanoparticle supported on carbon black (b,d). Both Pt NCs were captured along [01$\bar{1}$] zone axis, as indicated by the fast Fourier transform patterns (insets in c and d). Although both TEM profiles are hexagon, the lattice of the THH NCs along [111] and [100] directions (arrows) shrinks to a vertex; by contrast, the lattice of the cuboctahedral NCs tends to an edge.

the (111) and (100) lattices of the THH NC gradually shrink to a vertex (Figure 2c), which is consistent with the atomic model of THH NC (Figure 2a). That is, no {111} or {100} facets exist on the surfaces. These different behaviors confirm that the synthesized Pt NCs have a THH shape.

To understand the growth processes of the THH Pt NCs, we measured TEM images of samples prepared at different time of SWP treatment (Figure 3). The following processes occur during

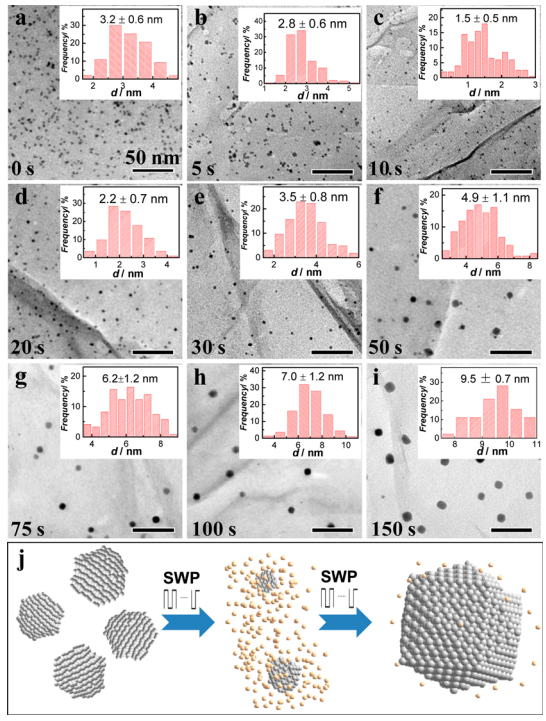

Figure 3. (a–i) TEM images and size histograms of Pt nanocrystals obtained at different time (0–150 s) of SWP treatment. (j) Illustration of the growth processes of THH Pt NCs from Pt nanoparticles. Gray spheres: metallic Pt atoms. Yellow spheres: Pt ions in the solution.

DOI: 10.1021/jacs.5b13473
J. Am. Chem. Soc. 2016, 138, 5753–5756

SWP treatment: (1) At E_U, oxygen species derived from H_2O dissociation can adsorb on Pt surface, and some Pt atoms can be dissolved into Pt ions. (2) At E_L, the oxygen species can be desorbed, and Pt ions in the solution can be reduced; as a result, the Pt NCs grow. During the SWP treatment, these processes occurred periodically. In Figure 3a–c, the size of Pt nanoparticles decreases from 3.2 to 1.5 nm in the first 10 s; the density of Pt nanoparticles also decreases. This result indicates that Pt nanoparticle dissolution dominates in the initial state. Along with Pt nanoparticle dissolution, the Pt ion concentration near electrode surface increases; this process promotes the growth of the survived Pt nanoparticles. Accordingly, the size of Pt nanoparticles increases after 10 s (Figure 3d–f). At 75 s, some faceted Pt NCs of 6.2 nm in size can be observed (Figure 3g). At 100 s, some Pt NCs with a regular shape appear (Figure 3h). At 150 s, most Pt NCs are converted into THH Pt NCs with an average size of 9.5 nm (Figure 3i). The morphological changes in the Pt nanoparticles can be also observed clearly in the HRTEM images (Figure S6). When the SWP treatment was prolonged to 200 s, large THH Pt NCs with a size of 12.2 nm can be obtained (Figure S7). According to the above results, electrochemically seed-mediated growth of THH Pt NCs can be illustrated in Figure 3j. It contains dissolution, growth, and surface reconstruction of Pt NCs. The key for the formation of high-index facets is the repetitive oxygen adsorption/desorption induced by SWP, which can result in place-exchange between oxygen and Pt surface atoms on low-index facets and then form step sites.[4,5] The support of graphene is not essential for the formation of high-index facets because the use of carbon black instead of graphene could also yield THH Pt NCs (Figure S8). Graphene was selected as substrate here because its TEM image has low contrast, which facilitates the observation of Pt lattice, especially the outmost-layer atoms in HRTEM characterization (Figure 2c).

In addition to the SWP, Pt seeds and dilute H_2PtCl_6 solution are also important for the growth of sub-10 nm THH Pt NCs. Without Pt nanoparticles as seeds, Pt NCs could not grow on graphene under SWP condition (Figure S9). If the SWP treatment was conducted in a 0.1 M H_2SO_4 solution without H_2PtCl_6 precursor, only spherical Pt nanoparticles of 4.9 nm were obtained (Figure S10). However, when H_2PtCl_6 concentration is higher than 10 μM, it is difficult to control the size of THH Pt NCs within 10 nm.

The as-synthesized THH-Pt/G catalyst exhibits a high catalytic activity for ethanol electrooxidation. Figure 4 depicts cyclic voltammograms of THH-Pt/G, Pt/G, and commercial Pt/C (10 *wt*.%) in 0.1 M ethanol + 0.1 M $HClO_4$ at 10 mV s^{-1}. The Pt loading used to calculate mass activity was determined by using inductively coupled plasma mass spectrometry (ICP-MS) just after the electrocatalytic test (Table S1). Therefore, the change of Pt mass during SWP treatment has been corrected. The ethanol electrooxidation yields two peaks in the forward scan. The first peak at 0.52 V can be attributed to ethanol oxidation on clean Pt surface, mainly yielding acetaldehyde and acetic acid, as well as slight CO_2; the second peak at 0.93 V mainly comes from ethanol oxidation on the oxidized Pt surface and produces acetic acid.[10] Considering the oxidation potential, only the first peak is relevant to direct ethanol fuel cells. Among the three catalysts, THH-Pt/G exhibits the highest catalytic activity, and its peak current density (j_p) in the forward scan is 0.52 A mg^{-1}, which is about 1.4 and 1.7 times higher than those of Pt/G and commercial Pt/C catalysts, respectively. We also evaluated the electrocatalytic activity of THH-Pt/G at different SWP treatment time (Figure S11). As the treatment time increases, the mass activity increases because of the formation of high-index facets and reaches a maximum at 150 s, and then decreases because of the formation of large NCs with low specific surface area.

This electrochemically seed-mediated method is also valid for reshaping commercial Pt/C catalyst to create high-index facets. The commercial Pt/C was subjected to electrochemical SWP (E_L = −0.30 V, E_U = 1.15 V, and f = 10 Hz) treatment in 0.1 M H_2SO_4 + 10 μM H_2PtCl_6 solution for 150 s, and the obtained sample was denoted as Pt/C_SWP. Figure 5a,b illustrates TEM images of commercial Pt/C catalyst before and after the SWP treatment. The particle size increases from 3.1 to 6.3 nm, and some faceted nanoparticles with a hexagonal projection along the ⟨110⟩ direction can be observed after the SWP treatment. The Miller index of the facet was identified as near {320} (Figure S12). Although the surface area decreases, the mass activity for ethanol electrooxidation still increases by 53% because the high active

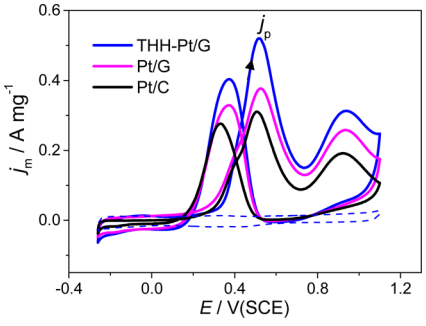

Figure 4. Cyclic voltammograms of THH-Pt/G, Pt/G, and commercial Pt/C at 10 mV s^{-1} in 0.1 M ethanol + 0.1 M $HClO_4$. The background curve of THH-Pt/G recorded in 0.1 M $HClO_4$ solution (dashed line) was also shown.

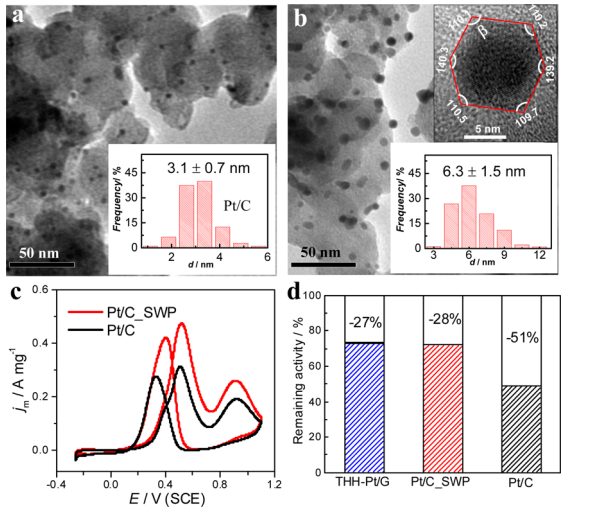

Figure 5. TEM images and size histograms of commercial Pt/C before (a) and after (b) electrochemical SWP treatment in 10 μM H_2PtCl_6 + 0.1 M H_2SO_4. HRTEM image of a Pt NC along ⟨110⟩ direction, showing a hexagonal profile, was inset in (b). (c) Cyclic voltammograms of commercial Pt/C before and after SWP treatment for ethanol oxidation in 0.1 M ethanol + 0.1 M $HClO_4$ at 10 mV s^{-1}. (d) Remaining activity of THH-Pt/G, Pt/C_SWP, and Pt/C for ethanol oxidation after 1000 potential cycles between −0.26 and 1.10 V at 100 mV s^{-1}.

DOI: 10.1021/jacs.5b13473
J. Am. Chem. Soc. 2016, 138, 5753–5756

high-index facets are formed on the Pt/C_SWP (Figure 5c). For surface area-specific activity, the Pt/C_SWP is approximately 2.7 times higher than the Pt/C (Figures S13 and S14). The catalytic activity of a catalyst depends on the shape, size, composition, and supports. THH-Pt/G and Pt/C_SWP have much higher surface area-specific activity than Pt/G and Pt/C, which may be correlated with the different surface structures and particle sizes. For ethanol electrooxidation on Pt, increasing particle size will decrease the surface area-specific activity when the particle size is larger than 2.5 nm.[11] So the higher surface area-specific activity of the THH-Pt/G and Pt/C_SWP than Pt/G and Pt/C is mainly attributed to the high-index facets. As for support effect, Pt/G and Pt/C has similar particle sizes, but the former has slightly higher catalytic activity than the latter. This result suggests that the graphene may promote slightly catalytic activity in comparison with carbon black.

Interestingly, Pt/C_SWP is more stable than Pt/C. This performance was evaluated by potential cycling between −0.26 and 1.10 V at 100 mV s^{-1} in 0.1 M ethanol + 0.1 M $HClO_4$ solution (Figure S15). After 1000 potential cycles, the Pt/C_SWP lost 28% of its initial activity. By contrast, Pt/C lost 51% of its activity (Figures 5d and S14). Pt-THH/G was also subjected to the same stability test, and lost its catalytic activity by 27%, but still maintained the THH shape (Figure S16). Note that high-index facets of THH Pt NCs have high stability because they are formed under a very harsh electrochemical environment. The SWP is similar to potential cycling for accelerated stability test. THH Pt NCs formed under SWP condition should have naturally high resistance to electrochemical corrosion.

In conclusion, this study provides new insight into the size- and shape-controlled synthesis of high-index faceted Pt NCs supported on carbon materials. In particular, graphene-supported THH Pt NCs with a size of sub-10 nm were prepared for the first time via the proposed electrochemically seed-mediated method. This method is also valid to reshape commercial Pt/C to create high-index facets. Thus, both mass activity and stability of Pt NCs have been enhanced.

■ ASSOCIATED CONTENT

Supporting Information

The Supporting Information is available free of charge on the ACS Publications website at DOI: 10.1021/jacs.5b13473.

Details of materials and methods as well as additional TEM images and electrochemical data (PDF)

■ AUTHOR INFORMATION

Corresponding Authors

*tnsd@xmu.edu.cn

*sgsun@xmu.edu.cn

Notes

The authors declare no competing financial interest.

■ ACKNOWLEDGMENTS

This work was supported by grants from Major State Basic Research Development Program of China (2012CB215500) and Natural Science Foundation of China (21222310, 21573183, 21361140374, and 21321062). This work made use of the resources of the National Center for Electron Microscopy in Beijing for Information Science and Technology.

■ REFERENCES

(1) Chen, A.; Holt Hindle, P. *Chem. Rev.* **2010**, *110*, 3767.

(2) Xia, Y. N.; Xiong, Y. J.; Lim, B.; Skrabalak, S. E. *Angew. Chem., Int. Ed.* **2009**, *48*, 60.

(3) Narayanan, R.; El Sayed, M. A. *J. Phys. Chem. B* **2005**, *109*, 12663.

(4) Tian, N.; Zhou, Z. Y.; Sun, S. G.; Ding, Y.; Wang, Z. L. *Science* **2007**, *316*, 732.

(5) (a) Zhou, Z. Y.; Tian, N.; Li, J. T.; Broadwell, I.; Sun, S. G. *Chem. Soc. Rev.* **2011**, *40*, 4167. (b) Zhou, Z. Y.; Shang, S. J.; Tian, N.; Wu, B. H.; Zheng, N. F.; Xu, B. B.; Chen, C.; Wang, H. H.; Xiang, D. M.; Sun, S. G. *Electrochem. Commun.* **2012**, *22*, 61.

(6) (a) Quan, Z.; Wang, Y.; Fang, J. *Acc. Chem. Res.* **2013**, *46*, 191. (b) Ming, T.; Feng, W.; Tang, Q.; Wang, F.; Sun, L.; Wang, J.; Yan, C. *J. Am. Chem. Soc.* **2009**, *131*, 16350. (c) Lin, H. X.; Lei, Z. C.; Jiang, Z. Y.; Hou, C. P.; Liu, D. Y.; Xu, M. M.; Tian, Z. Q.; Xie, Z. X. *J. Am. Chem. Soc.* **2013**, *135*, 9311.

(7) Zhang, H.; Jin, M. S.; Xia, Y. N. *Angew. Chem., Int. Ed.* **2012**, *51*, 7656.

(8) Sun, Y.; Zhuang, L.; Lu, J.; Hong, X.; Liu, P. *J. Am. Chem. Soc.* **2007**, *129*, 15465.

(9) Xiao, J.; Liu, S.; Tian, N.; Zhou, Z. Y.; Liu, H. X.; Xu, B. B.; Sun, S. G. *J. Am. Chem. Soc.* **2013**, *135*, 18754.

(10) (a) Li, N. H.; Sun, S. G.; Chen, S. P. *J. Electroanal. Chem.* **1997**, *430*, 57. (b) Heinen, M.; Jusys, Z.; Behm, R. J. *J. Phys. Chem. C* **2010**, *114*, 9850. (c) Leung, L.W. H.; Chang, S. C.; Weaver, M. J. *J. Electroanal. Chem. Interfacial Electrochem.* **1989**, *266*, 317.

(11) Perez, J.; Paganin, V. A.; Antolini, E. *J. Electroanal. Chem.* **2011**, *654*, 108.

DOI: 10.1021/jacs.5b13473
J. Am. Chem. Soc. 2016, 138, 5753−5756